

Selenoglycosides as Lectin Ligands: ^{77}Se -Edited CPMG-HSQMBC NMR Spectroscopy To Monitor Biomedically Relevant Interactions

Mária Raics,^[a] István Timári,^[a] Tammo Diercks,^[b] László Szilágyi,^[c] Hans-Joachim Gabius,^{*,[d]} and Katalin E. Kövér^{*,[a]}

The fundamental importance of protein–glycan recognition calls for specific and sensitive high-resolution techniques for their detailed analysis. After the introduction of ^{19}F NMR spectroscopy to study the recognition of fluorinated glycans, a new ^{77}Se NMR spectroscopy method is presented for complementary studies of selenoglycans with optimised resolution and sensitivity, in which direct NMR spectroscopy detection on ^{77}Se is replaced by its indirect observation in a 2D $^1\text{H},^{77}\text{Se}$ HSQMBC spectrum. In contrast to OH/F substitution, O/Se exchange allows the glycosidic bond to be targeted. As an example, selenodigalactoside recognition by three human galectins and a plant toxin is readily indicated by signal attenuation and line broadening in the 2D $^1\text{H},^{77}\text{Se}$ HSQMBC spectrum, in which CPMG-INEPT long-range transfer ensures maximal detection sensitivity, clean signal phases, and reliable ligand ranking. By monitoring competitive displacement of a selenated spy ligand, the selective ^{77}Se NMR spectroscopy approach may also be used to screen non-selenated compounds. Finally, $^1\text{H},^{77}\text{Se}$ CPMG-INEPT transfer allows further NMR sensors of molecular interaction to be combined with the specificity and resolution of ^{77}Se NMR spectroscopy.

Glycans are increasingly recognised for their capacity to encode biological information at high density, thus attracting interest in understanding how it is specifically read and trans-

lated into a plethora of physiological effects.^[1] For instance, the recognition of cellular glycoconjugates by various endogenous sugar receptors^[2] underlies specific bridging in the cell–cell/matrix adhesion and initiation of signalling in diverse regulatory processes such as the induction of anoikis/apoptosis, or mediator release in degenerative and inflammatory diseases like (osteo)arthritis.^[3] The analysis of such clinically relevant molecular recognition processes and screening for potent antagonists with maximal specificity, sensitivity, and resolution are still great experimental challenges on the way to cracking the sugar code and its biomedical implications.^[2c,4]


Solution-state NMR spectroscopy can probe molecular interactions with atomic resolution over a wide range of affinities,^[5] and NMR screening is now widely used in pharmaceutical research. It may be implemented with detection of suitable proteins, which requires their isotopic labelling, evinces binding sites, and includes irreversible binding. Alternatively, the unlabelled small ligands are observed, which allows faster throughput by pooling and spectrally separating compounds, and thus, is particularly suited to detect weak binding, but often overlooks strong binding because only the dissociated state is detected. Inherent problems of ^1H NMR spectroscopy, where signals often show poor dispersion, complex fine structure (from extensive homonuclear $J(\text{H},\text{H})$ coupling), and overlap (aggravated by a vast spectral background and intense solvent signals), further complicate ligand identification, especially in mixtures of chemically related compounds. These shortcomings are avoided upon selecting another NMR-active nucleus with superior signal dispersion and no natural background, which may be introduced by chemical derivation. For glycans with their particularly complex and similar ^1H NMR spectra,^[6] the substitution of hydroxyl groups for fluorine or oxygen for selenium atoms are established modifications, for example, to inhibit enzymatic degradation. This also introduces the extremely well dispersed spin- $1/2$ NMR isotopes ^{19}F and ^{77}Se , with chemical shift ranges of $\delta \approx 300$ and 3000 ppm, respectively. For ^{19}F , high natural abundance (100%) and sensitivity (83% of ^1H) facilitate direct NMR detection and have boosted the development and broad application of diverse ^{19}F NMR spectroscopy techniques for efficient screening and detailed analysis of molecular interactions.^[7] For the rare (7.63% abundance) and insensitive (0.7% of ^1H) ^{77}Se isotope,^[8] in contrast, direct ^{77}Se NMR detection^[9] is unfavourable. To enhance the sensitivity substantially and enable reliable ligand ranking by affinities, we propose indirect ^{77}Se detection and initial $^1\text{H} \rightarrow ^{77}\text{Se}$ polar-


[a] M. Raics, Dr. I. Timári, Prof. Dr. K. E. Kövér
Department of Inorganic and Analytical Chemistry, University of Debrecen
Egyetem tér 1, 4032 Debrecen (Hungary)
E-mail: kover@science.unideb.hu

[b] Dr. T. Diercks
NMR Facility, CIC bioGUNE
Bizkaia Technology Park, Bld 800, 48170 Derio (Spain)

[c] Prof. Dr. L. Szilágyi
Department of Organic Chemistry, University of Debrecen
Egyetem tér 1, 4032 Debrecen (Hungary)

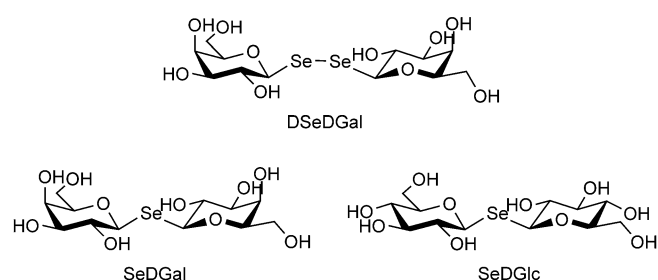
[d] Prof. Dr. H.-J. Gabius
Tierärztliche Fakultät, Institut für Physiologische Chemie
Ludwig-Maximilians-Universität München
Veterinärstrasse 13, 80539 Munich (Germany)
E-mail: gabius@tiph.vetmed.uni-muenchen.de

 Supporting information and the ORCID identification numbers for the authors of this article can be found under <https://doi.org/10.1002/cbic.201900088>.

 © 2019 The Authors. Published by Wiley-VCH Verlag GmbH & Co. KGaA. This is an open access article under the terms of the Creative Commons Attribution Non-Commercial License, which permits use, distribution and reproduction in any medium, provided the original work is properly cited and is not used for commercial purposes.

sation transfer, as implemented in the 2D ^1H , ^{77}Se HSQMB C experiment with CPMG-INEPT out-and-back transfer.

Despite great success, broad applications, and the advanced technical state of ^{19}F NMR based interaction studies, analogous ^{77}Se NMR approaches may become an important complementary technique because the required OH/F and O/Se substitutions label different molecular sites for NMR observation and with distinct biochemical impacts. In particular, whereas OH/F substitution removes a potential hydrogen-bond donor that may impair or even abolish molecular recognition, O/Se exchange in the glycosidic bond has no known adverse effects, but increases its stability against hydrolysis. Several previous findings indicate that selenoglycosides are excellent biomimetics of natural O-glycosides and exhibit similar dynamic and conformational properties to those of thioglycosides,^[10] whereas molecular docking analyses predict full biocompatibility with O-glycosides.^[11] Methyl selenoglycosides co-crystallise readily with their cognate bacterial, fungal, and human lectins to enable multi-wavelength anomalous diffraction (MAD) phasing of their complex crystal structures.^[12] The diselenodiglycoside of β -GlcNAc was shown to be a ligand for wheat germ agglutinin by means of ^1H saturation transfer difference (STD) NMR spectroscopy, whereas its presence in serum was traced by means of ^{77}Se NMR spectroscopy.^[13] Similar to their thio analogues,^[10,14] selenodigalactoside (SeDGal; Scheme 1) and diselenodigalactoside (DSeDGal) were recognised by human galectins and a ricin-like plant toxin,^[15] in contrast to diselenodigalactoside (DSeDGLc). At the same time, selenoglycoside synthesis^[16] has advanced greatly, and ^{77}Se NMR signal shifts were shown to be sensitive indicators for phenylselenenyl acetate binding to α -chymotrypsin^[17] and selenomethyl glycoside binding to plant lectins.^[9] All studies, however, employed very insensitive direct ^{77}Se NMR detection.



Scheme 1. Structures of the selenodiglycosides used in this study.

To further explore the NMR spectroscopy potential of selenated compounds far more efficiently, we herein propose indirect ^{77}Se detection through ^1H and initial $^1\text{H} \rightarrow ^{77}\text{Se}$ polarisation transfer to increase the sensitivity by $12 = (\gamma_{\text{H}}/\gamma_{^{77}\text{Se}})^{3/2}$ and $5.23 = (\gamma_{\text{H}}/\gamma_{^{77}\text{Se}})$, respectively, that is, by a factor of 63 overall. Yet, the approach relies on moderate scalar two- and three-bond $^{2,3}J(\text{H}, ^{77}\text{Se})$ couplings (10–30 Hz) for out-and-back transfer of ^1H coherence to a ^{77}Se spin in the glycosidic bond that require rather long transfer periods $2\Delta \approx (^{2,3}J(\text{H}, ^{77}\text{Se}))^{-1} = 30$ –100 ms. Transfer efficiency is then degraded by transverse ^1H

R_2 relaxation and by competing evolution of homonuclear $J(\text{H}, \text{H})$ coupling that causes periodic signal phase and amplitude modulation. The use of CPMG-INEPT^[18] for $^1\text{H} \rightarrow ^{77}\text{Se}$ coherence transfer can alleviate these deleterious effects of COSY-type $J(\text{H}, \text{H})$ evolution by enforcing TOCSY-type evolution instead, which is purely in-phase and eventually leads to equipartition of magnetisation in the coupled ^1H spin system. This removes signal phase modulation and greatly reduces intensity losses from co-evolving $J(\text{H}, \text{H})$ coupling. Moreover, CPMG-INEPT can suppress line broadening from chemical exchange (R_{exch}) that often increases the net ^1H R_2^* relaxation rate in cases of transient interactions provided that the CPMG echo delay (τ in Figure 1) is shorter than the lifetime of interchanging states (τ_{exch}).^[19] If this condition is maintained for all ligands binding to the same site of a protein, relaxation losses are minimised and R_2^* is reduced to a population-weighted sum of slow $R_{2,\text{f}}$ and fast $R_{2,\text{b}}$ relaxation rates for the free (f) and bound (b) ligand state, respectively [Eq. (1)]:

$$R_2^* = p_{\text{f}}R_{2,\text{f}} + p_{\text{b}}R_{2,\text{b}} = R_{2,\text{f}} + p_{\text{b}}(R_{2,\text{protein}} - R_{2,\text{f}}) \quad (1)$$

For small ligands ($R_{2,\text{f}} \ll R_{2,\text{protein}}$) in the weak binding regime ($p_{\text{b}} \approx K_{\text{A}}$), R_2^* then becomes proportional to the affinity constant, K_{A} [Eq. (2)]:

$$R_2^* \approx R_{2,\text{f}} + K_{\text{A}}R_{2,\text{protein}} \quad (2)$$

Thus, the signal intensity (I) of a ligand in the presence of a weakly binding protein is attenuated according to Equa-

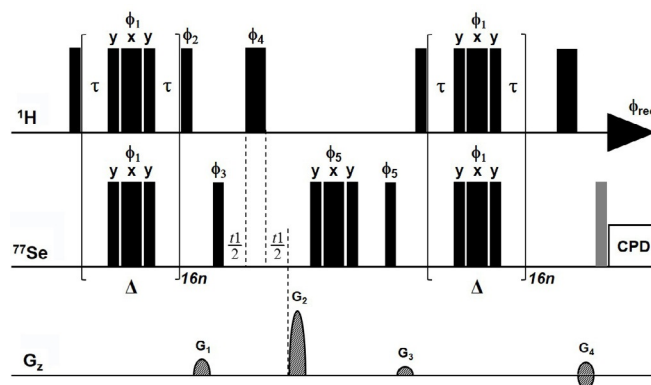


Figure 1. Pulse sequence of the 2D ^1H , ^{77}Se CPMG-HSQMB C experiment. Narrow and broad bars indicate 90 and 180° pulses, respectively, applied with phase x, unless indicated otherwise. φ_1 is incremented according to the XY16 scheme^[20] used in the CPMG-INEPT module. Further phases: $\varphi_2 = y$; $\varphi_3 = x, -x$; $\varphi_4 = x, x, -x, -x$; $\varphi_5 = x, x, x, x, -x, -x, -x, -x$; $\varphi_{\text{rec}} = x, -x, x, -x, -x, x, -x, x$. The last 90° pulse on ^{77}Se (grey) is an optional clean in-phase (CLIP) purge pulse^[21] to destroy residual $2\text{H}_{\text{N}}\text{Se}$ anti-phase components. The CPMG echo delay, τ , was set to 150 μs , while the number, n , of CPMG echos was adjusted to achieve the desired $^{2,3}J(\text{H}, ^{77}\text{Se})$ coupling evolution time, $\Delta \leq 0.5^{2,3}J(\text{H}, ^{77}\text{Se})$. Clean, phase-sensitive ^{77}Se coherence selection is achieved by setting gradient pulse strengths $G_2/G_4 = 80: \pm 15.257$ (with alternating sign between serial free induction decays (FIDs)). The z-spoil gradients G_1 and G_3 have arbitrary but distinct strengths. Sine bell-shaped gradient pulses of 1 ms duration were followed by a recovery delay of 200 μs . For ^{77}Se composite pulse decoupling (CPD) during FID acquisition, the WALTZ16 (or 64) scheme with a 90° pulse length of 0.5/BW (^{77}Se) was used, in which BW is the bandwidth [Hz] of the ^{77}Se spectrum.

tion (3):

$$I \propto \exp(-2\Delta[R_{2f} + K_A R_{2,\text{protein}}]) \quad (3)$$

whereas the intensity in the absence of the protein (I_0) is attenuated only by slow R_{2f} relaxation [Eq. (4)]:

$$I_0 \propto \exp(-2\Delta R_{2f}) \quad (4)$$

The R_{2f} dependence then cancels out in the ratio of the signal intensity of a ligand in the presence and absence of a cognate protein [Eq. (5)]:

$$I/I_0 \approx \exp(-2\Delta K_A R_{2,\text{protein}}) \quad (5)$$

Thus, relative signal attenuations from binding allow a ranking of two ligands, a and b, that bind to the same site of a protein, and an estimation of the ratio of their affinity constants [Eq. (6)]:

$$K_{A,a}/K_{A,b} \approx \ln(I/I_0)_a / \ln(I/I_0)_b \quad (6)$$

This approximation holds for small ligands in the weak binding regime [Eq. (2)] if line broadening from chemical exchange (R_{exch}) is suppressed. By ensuring this as well as undistorted signal shapes, CPMG-INEPT enhances sensitivity and is critical for reliable ligand ranking by relative affinities. Nevertheless, R_{exch} is not suppressed during chemical shift evolution, thus adding to R_2^* relaxation [Eq. (2)] of ^{77}Se (t_1) and ^1H (t_2) as extra line broadening. Although this enhances indication sensitivity for molecular interactions, it biases signal intensities, but not their integrals. Thus, Equations (4) to (6) strictly apply to signal integrals, but are also approximately valid for signal intensities.

The 2D ^1H , ^{77}Se CPMG-HSQMBC (Figure 1) is derived from our previously presented 2D CPMG-HSQMBC experiment with composite 90°_y – 180°_x – 90°_y inversion pulses for increased CPMG bandwidth at reduced power and clean coherence selection by echo/antiecho gradients (G_2 , G_4).^[22] Contrary to the original experiment, which was developed to accurately measure long-range coupling constants, a refocusing second CPMG-INEPT module is inserted prior to FID acquisition to enable ^{77}Se decoupling in order to obtain sharp and purely in-phase signals for easy quantification of signal intensities or integrals.

A 2D ^1H , ^{77}Se HSQMBC spectrum of SeDGal and DSeDGal (Figure 2) illustrates the significant phase distortions (in the ^1H dimension) and sensitivity losses due to amplitude modulation from COSY-type co-evolution of homonuclear $^nJ(\text{H,H})$ couplings during conventional INEPT transfer. In contrast, CPMG-INEPT suppresses these deleterious effects and allows a quantitative analysis of the substantially enhanced signal intensities.

We then recorded 2D ^1H , ^{77}Se CPMG-HSQMBC spectra to analyse binding of SeDGal, DSeDGal, and SeDGLc (Scheme 1) to three human galectins and to *Viscum album* agglutinin (VAA). Both selenogalactosides show distinct signal attenuation after addition to Gal-3, an anti-apoptotic and pro-inflammatory effector and Gal-1 antagonist,^[16] at a molar excess of 20:1

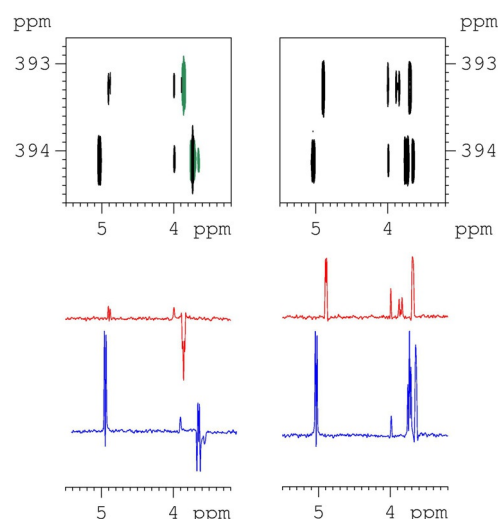


Figure 2. The 2D ^1H , ^{77}Se HSQMBC spectra of DSeDGal (red, 10 mM) and SeDGal (blue, 10 mM), implemented with INEPT (left) or CPMG-INEPT (right) modules. The $^1\text{H} \rightarrow ^{77}\text{Se}$ polarisation transfer delay, Δ , was set to 54.5 ms. The 1D ^1H (F2) traces extracted at both ^{77}Se resonances are shown below the contour plots to illustrate the suppression of signal phase and amplitude modulation from co-evolution of $J(\text{H,H})$ couplings during 2Δ afforded by CPMG-INEPT. Both spectra were recorded and plotted with identical parameters.

(Figure 3, right, top) or 60:1 (Figure 3, right, bottom). The extracted ^1H [^{77}Se] traces readily show strong signal attenuation for SeDGal (blue: $I/I_0 \approx 8\%$ at 20:1 molar ratio) and weak attenuation for DSeDGal (red: $I/I_0 \approx 84\%$ at 20:1 molar ratio), whereas the SeDGLc signals (black) remain unaffected. The extent of binding-induced signal attenuations agree well with previously reported IC_{50} values,^[15a] and Equation (6) suggests about 15-fold higher affinity for SeDGal than for DSeDGal. In the presence of Gal-1 (Figure S1 in the Supporting Information), the signal attenuations for SeDGal (at 20:1 molar ratio: $I/I_0 \approx 10\%$) and DSeDGal ($I/I_0 \approx 90\%$) are very similar to those caused by Gal-3, thus confirming a similar differential, albeit somewhat weaker, recognition by this related human galectin. In contrast, Gal-7 (Figure S2) provokes less attenuation of SeDGal signals (at 20:1 molar ratio: $I/I_0 \approx 36\%$), whereas DSeDGal signals are again attenuated only weakly ($I/I_0 \approx 92\%$), thus suggesting that Gal-7 discriminates less between SeDGal and DSeDGal than Gal-1 or Gal-3. Finally, VAA causes comparable signal attenuation for SeDGal and DSeDGal (Figure S3: $I/I_0 \approx 22$ and 27% , respectively), which confirms a very similar affinity of VAA for these two ligands, in contrast to the galectins.^[15] As a negative control, none of the four lectins affected SeDGLc signal intensities, in line with their specific galactose, but not glucose, recognition. In summary, induced signal attenuations observed in 2D ^1H , ^{77}Se CPMG-HSQMBC spectra appear to be a valid indicator of ligand binding and allow their reliable ranking by relative affinities.

Our experiments with mixtures of three selenoglycosides implicitly register their competitive displacement if they share a common binding site. To verify this assumption, we also recorded signal attenuations in the 2D ^1H , ^{77}Se CPMG-HSQMBC spectrum after addition of only DSeDGal (2.5 mM) to a lectin

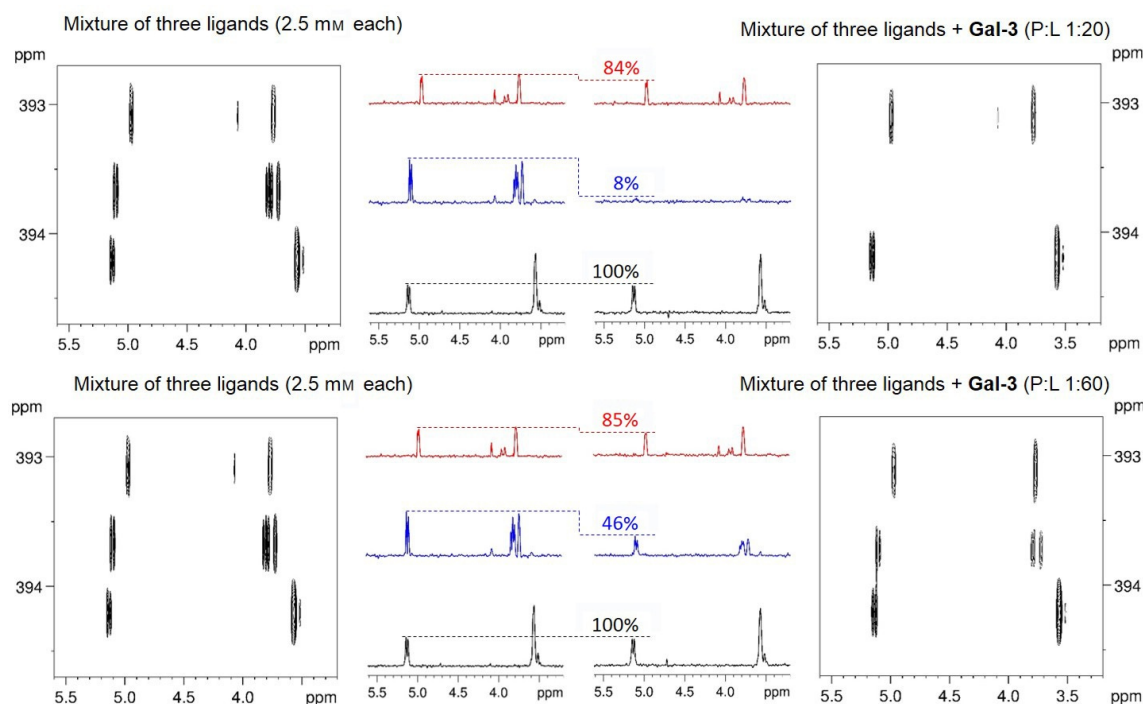


Figure 3. Selenoglycoside binding to Gal-3 monitored by 2D ^1H , ^{77}Se CPMG-HSQMBC. The 2D spectra of the ligand mixture containing DSeDGal (red), SeDGal (blue), and SeDGlc (black) at 2.5 mM concentrations each were recorded before (left) and after (right) adding Gal-3 to a protein/ligand ratio of 1:20 (top) and 1:60 (bottom). ^1H (F2) traces extracted at the three ^{77}Se signals are shown next to the contour plots. The indicated attenuated signal intensities from binding are relative to the free ligand intensity. Each 2D ^1H , ^{77}Se CPMG-HSQMBC spectrum was measured and plotted with identical parameters. Further experimental details can be found in the Supporting Information.

(125 μM ; 30 μM for Gal-3 to avoid its precipitation), and after subsequent coaddition of SeDGal (2.5 mM). The latter caused a significant rebound of the DSeDGal signal attenuation (I/I_0) with all four test lectins, that is, from 55 to 91% for Gal-1 (Figure S4), 67 to 86% for Gal-3 (Figure 4), 89 to 97% for Gal-7 (Figure S5), and 12 to 37% for VAA (Figure S4). Thus, SeDGal displaces DSeDGal from all four lectins, which confirms their competitive binding at the same recognition site. This makes DSeDGal a suitable spy ligand to indirectly monitor galectin binding by means of 2D ^1H , ^{77}Se CPMG-HSQMBC through its competitive displacement, which allows application of this specific and sensitive detection method to be extended to non-selenated compounds as well. In such assays with a single selenated spy ligand, the 1D version of the experiment, that is, a ^1H [^{77}Se -filtered] CPMG-HSQMBC, should be more efficient than the 2D version. However, the latter is generally preferable for mixtures of selenated compounds to resolve ^1H signal overlap as the most important source of information bias or loss.

The proposed HSQMBC scheme for indirect ^{77}Se detection with initial $^1\text{H} \rightarrow ^{77}\text{Se}$ polarisation transfer by CPMG-INEPT may easily be combined with other sensors of molecular interaction than the signal attenuation (from increased R_2 relaxation) exploited here. For instance, intermolecular $^1\text{H}_{\text{protein}} \rightarrow ^1\text{H}_{\text{ligand}}$ saturation transfer can be combined with the extreme spectral resolution, clarity, and specificity of ^{77}Se editing in a 2D STD- ^1H , ^{77}Se -HSQMBC experiment in order to study transient molecular interactions without spectral background and artefacts. For analyses of stable protein–ligand complexes, the same

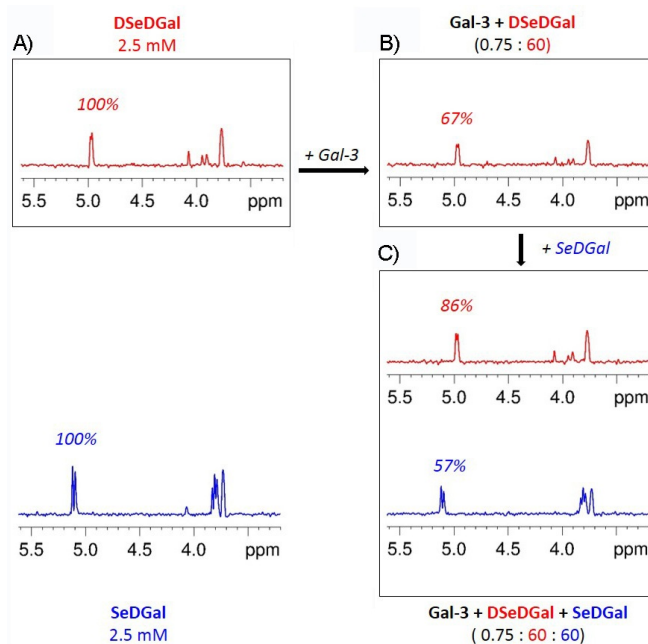


Figure 4. Competitive displacement of diselenodigalactoside (DSeDGal) binding to Gal-3, monitored by 2D ^1H , ^{77}Se CPMG-HSQMBC. A) ^1H (F2) traces of DSeDGal (red, top) and SeDGal (blue, bottom) in the absence of Gal-3, yielding the reference signal intensities, $I_0 = 100\%$. B) The ^1H (F2) trace of DSeDGal (2.5 mM) after adding Gal-3 (30 μM , that is, molar ratio = 0.75:60) reveals a binding-induced signal attenuation to $I/I_0 = 67\%$. C) Equimolar addition of SeDGal (2.5 mM) causes a rebound of the attenuated DSeDGal signal to 86% (red, top), thus indicating its competitive displacement. The SeDGal spectrum is conversely attenuated to 57% (blue, bottom), which confirms its preferred binding by Gal-3.

CPMG-HSQMBC building block may be used, for example, in a diagonal free 2D $^1\text{H}[^{13}\text{C}], ^1\text{H}[^{77}\text{Se}]$ NOESY experiment to specifically observe intermolecular NOE contacts between a ^{13}C -labelled protein and a selenated ligand.

In conclusion, we have presented an optimised general scheme for the specific study of selenated compounds by means of ^{77}Se NMR spectroscopy, with substantially increased sensitivity and resolution compared with that of the previously proposed direct 1D ^{77}Se detection method.^[9] The proposed 2D $^1\text{H}, ^{77}\text{Se}$ CPMG-HSQMBC experiment instead detects ^{77}Se indirectly in a second spectral dimension, by employing $^1\text{H} \rightarrow ^{77}\text{Se}$ CPMG-INEPT out-and-back transfer through $^{2,3}\text{J}(\text{H}, ^{77}\text{Se})$ long-range coupling. As shown for the example of selenoglycoside recognition by three clinically relevant human galectins and the plant toxin VAA, this experiment enables efficient screening of selenated ligands, sensitive detection of molecular binding, and reliable ligand ranking by relative affinities. The range of applications is vast and similar to that of ^{19}F NMR-based techniques, whereas selenium introduction through O/Se exchange has far less potential impact on molecular interactions and can target other sites than OH/F exchange. This may be particularly important and beneficial in glycosciences, where O/Se exchange in the glycosidic bond is now well established and allows glycan/protein recognition to be studied directly at this often critical linkage, and without risk of impairing molecular interactions, in contrast to OH/F exchange.

Acknowledgements

This research was supported by the National Research, Development and Innovation Office of Hungary (grant NKFI/ OTKA NN 128368) and co-financed by the European Regional Development Fund (projects GINOP-2.3.3-15-2016-00004, GINOP-2.3.2-15-2016-00044, and GINOP-2.3.2-15-2016-00008). We also thank Drs. Brian Friday, Alfred Leddoz, and Albert W. L. Nose for inspiring discussions.

Conflict of Interest

The authors declare no conflict of interest.

Keywords: glycosides • lectins • molecular recognition • NMR spectroscopy • selenium

- [1] a) P. J. Winterburn, C. F. Phelps, *Nature* **1972**, 236, 147; b) R. A. Laine in *Glycosciences: Status and Perspectives* (Eds.: H.-J. Gabius, S. Gabius), Chapman & Hall, London, **1997**, p. 1; c) H.-J. Gabius, H.-C. Siebert, S. Andry, J. Jiménez-Barbero, H. Rüdiger, *ChemBioChem* **2004**, 5, 740; d) H.-J. Gabius, J. Roth, *Histochem. Cell Biol.* **2017**, 147, 111.
- [2] a) H. Lis, N. Sharon, *Chem. Rev.* **1998**, 98, 637; b) J. C. Manning, A. Romero, F. A. Habermann, G. García Caballero, H. Kaltner, H.-J. Gabius, *Histochem. Cell Biol.* **2017**, 147, 199; c) H. Kaltner, G. García Caballero, A.-K. Ludwig, J. C. Manning, H.-J. Gabius, *Histochem. Cell Biol.* **2018**, 149, 547.
- [3] a) F. L. Harrison, C. J. Chesterton, *FEBS Lett.* **1980**, 122, 157; b) D. Solís, N. V. Bovin, A. P. Davis, J. Jiménez-Barbero, A. Romero, R. Roy, K. Smetana, Jr., H.-J. Gabius, *Biochim. Biophys. Acta* **2015**, 1850, 186; c) H. Kaltner, S. Toegel, G. García Caballero, J. C. Manning, R. W. Ledeen, H.-J. Gabius, *Histochem. Cell Biol.* **2017**, 147, 239; d) S. Mayer, M. K. Raulf, B. Lepenies, *Histochem. Cell Biol.* **2017**, 147, 223; e) D. Weinmann, M. Kenn, S. Schmidt, K. Schmidt, S. M. Walzer, B. Kubista, R. Windhager, W. Schreiner, S. Toegel, H.-J. Gabius, *Cell. Mol. Life Sci.* **2018**, 75, 4187; f) Q. Xiao, A.-K. Ludwig, C. Romanò, I. Buzzacchera, S. E. Sherman, M. Vetro, S. Vértessy, H. Kaltner, E. H. Reed, M. Möller, C. J. Wilson, D. A. Hammer, S. Oscarson, M. L. Klein, H.-J. Gabius, V. Percec, *Proc. Natl. Acad. Sci. USA* **2018**, 115, E2509; g) A.-K. Ludwig, M. Michalak, Q. Xiao, U. Gilles, F. J. Medrano, H. Ma, F. G. FitzGerald, W. D. Hasley, A. Melendez-Davila, M. Liu, K. Rahimi, N. Yu Kostina, C. Rodriguez-Emmenegger, M. Möller, I. Lindner, H. Kaltner, M. Cudic, D. Reusch, J. Kopitz, A. Romero, S. Oscarson, M. L. Klein, H.-J. Gabius, V. Percec, *Proc. Natl. Acad. Sci. USA* **2019**, 116, 2837.
- [4] H.-J. Gabius, *Folia Biol.* **2017**, 63, 121.
- [5] a) T. Diercks, M. Coles, H. Kessler, *Curr. Opin. Chem. Biol.* **2001**, 5, 285; b) O. Cala, F. Guilliery, I. Krimm, *Anal. Bioanal. Chem.* **2014**, 406, 943; c) B. Walter, B. K. Chaitanya, G. Nina, Z. Klaus, *ChemPhysChem* **2018**, 19, 895; d) A. Ardá, J. Jiménez-Barbero, *Chem. Commun.* **2018**, 54, 4761.
- [6] K. E. Kövér, L. Szilágyi, G. Batta, D. Uhrin, J. Jiménez-Barbero, *Comprehensive Natural Products II, Chemistry and Biology*, Vol. 9 (Eds.: L. Mander, H.-W. Liu), Elsevier, Oxford, **2010**, pp. 197.
- [7] a) C. Dalvit, *Progr. Nucl. Magn. Reson. Spectrosc.* **2007**, 51, 243; b) J. P. Ribeiro, T. Diercks, J. Jiménez-Barbero, S. André, H.-J. Gabius, F. J. Cañada, *Biomolecules* **2015**, 5, 3177; c) T. Diercks, A. S. Infantino, L. Unione, J. Jiménez-Barbero, S. Oscarson, H.-J. Gabius, *Chem. Eur. J.* **2018**, 24, 15761.
- [8] H. Duddeck, *Annu. Rep. NMR Spectrosc.* **2004**, 52, 105.
- [9] C. Hamark, J. Landström, G. Widmalm, *Chem. Eur. J.* **2014**, 20, 13905.
- [10] S. André, Z. Pei, H.-C. Siebert, O. Ramström, H.-J. Gabius, *Bioorg. Med. Chem.* **2006**, 14, 6314.
- [11] F. Strino, J. H. Lii, C. A. Koppisetty, P. G. Nyholm, H.-J. Gabius, *J. Comput.-Aided Mol. Des.* **2010**, 24, 1009.
- [12] a) L. Buts, R. Loris, E. De Genst, S. Oscarson, M. Lahmann, J. Messens, E. Brosens, L. Wyns, H. De Greve, J. Bouckaert, *Acta Crystallogr. Sect. D Biol. Crystallogr.* **2003**, 59, 1012; b) J. Shimabukuro, H. Makyio, T. Suzuki, Y. Nishikawa, M. Kawasaki, A. Imamura, H. Ishida, H. Ando, R. Kato, M. Kiso, *Bioorg. Med. Chem.* **2017**, 25, 1132.
- [13] I. Pérez-Victoria, O. Boutureira, T. D. W. Claridge, B. G. Davis, *Chem. Commun.* **2015**, 51, 12208.
- [14] S. Martín-Santamaría, S. André, E. Buzamet, R. Caraballo, G. Fernández-Cureses, M. Morando, J. P. Ribeiro, K. Ramírez-Gualito, B. de Pascual-Teresa, F. J. Cañada, M. Menéndez, O. Ramström, J. Jiménez-Barbero, D. Solís, H.-J. Gabius, *Org. Biomol. Chem.* **2011**, 9, 5445.
- [15] a) S. André, K. E. Kövér, H.-J. Gabius, L. Szilágyi, *Bioorg. Med. Chem. Lett.* **2015**, 25, 931; b) H. Kaltner, T. Szabó, K. Fehér, S. André, S. Balla, J. C. Manning, L. Szilágyi, H.-J. Gabius, *Bioorg. Med. Chem.* **2017**, 25, 3158.
- [16] a) G. Wagner, P. Nuhn, *Arch. Pharm.* **1964**, 297, 461; b) A. A. Kumar, T. Z. Illyés, K. E. Kövér, L. Szilágyi, *Carbohydr. Res.* **2012**, 360, 8; c) T. Z. Illyés, S. Balla, A. Bényei, A. A. Kumar, I. Timári, K. E. Kövér, L. Szilágyi, *Chemistry-Select* **2016**, 1, 2383.
- [17] G. P. Mullen, R. B. Dunlap, J. D. Odom, *J. Am. Chem. Soc.* **1985**, 107, 7187.
- [18] a) H. Koskela, I. Kolpelainen, S. Halkinen, *J. Magn. Reson.* **2003**, 164, 228; b) K. E. Kövér, G. Batta, K. Fehér, *J. Magn. Reson.* **2006**, 181, 89.
- [19] a) K. Pervushin, V. Gallius, C. Ritter, *J. Biomol. NMR* **2001**, 21, 161; b) A. Zhuravleva, V. Y. Orekhov, *J. Am. Chem. Soc.* **2008**, 130, 3260.
- [20] T. Gullion, D. B. Baker, M. S. Conradi, *J. Magn. Reson.* **1990**, 89, 479.
- [21] a) O. W. Sørensen, R. R. Ernst, *J. Magn. Reson.* **1983**, 51, 477; b) A. Enthart, J. C. Freudenberger, J. Furrer, H. Kessler, B. Luy, *J. Magn. Reson.* **2008**, 192, 314.
- [22] a) S. Boros, K. E. Kövér, *Magn. Reson. Chem.* **2011**, 49, 106; b) I. Timári, L. Szilágyi, K. E. Kövér, *Chem. Eur. J.* **2015**, 21, 13939; c) I. Timári, K. E. Kövér, *Magn. Reson. Chem.* **2018**, 56, 910.

Manuscript received: February 11, 2019

Accepted manuscript online: March 3, 2019

Version of record online: June 5, 2019